

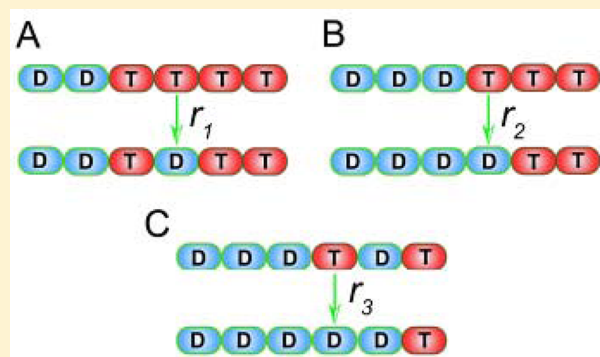
Theoretical Analysis of Microtubules Dynamics Using a Physical–Chemical Description of Hydrolysis

Xin Li and Anatoly B. Kolomeisky*

Department of Chemistry, Rice University, Houston, Texas 77005, United States

Supporting Information

ABSTRACT: Microtubules are cytoskeleton multifilament proteins that support many fundamental biological processes such as cell division, cellular transport, and motility. They can be viewed as dynamic polymers that function in nonequilibrium conditions stimulated by hydrolysis of GTP (guanosine triphosphate) molecules bound to their monomers. We present a theoretical description of microtubule dynamics based on discrete-state stochastic models that explicitly takes into account all relevant biochemical transitions. In contrast to previous theoretical analysis, a more realistic physical–chemical description of GTP hydrolysis is presented, in which the hydrolysis rate at a given monomer depends on the chemical composition of the neighboring monomers. This dependence naturally leads to a cooperativity in the hydrolysis. It is found that this cooperativity significantly influences all dynamic properties of microtubules. It is suggested that the dynamic instability in cytoskeleton proteins might be observed only for weak cooperativity, while the strong cooperativity in hydrolysis suppresses the dynamic instability. The presented microscopic analysis is compared with existing phenomenological descriptions of hydrolysis processes. Our analytical calculations, supported by computer Monte Carlo simulations, are also compared with available experimental observations.



INTRODUCTION

Cytoskeleton proteins such as microtubules and actin filaments are protein molecules that play a critical role in important biological processes including cell division, cytoplasmic organization, cellular transport, and motility.^{1–4} One of the most unusual properties of microtubules is a phenomenon known as dynamic instability, in which microtubules can be found in growing or shrinking dynamic phases that alternate stochastically.⁵ In recent years significant experimental advances in investigation of cellular processes have been achieved. It is now possible to visualize microscopic details of cytoskeletal protein assembly and dynamics with unprecedented nanometer precision and high temporal resolution.^{6–8} These experimental successes stimulated multiple theoretical efforts to understand cytoskeleton processes, which led to explanation of some properties of microtubules and actin filaments.^{9–17} However, underlying mechanisms of dynamic processes in cytoskeleton proteins remain not fully understood.

Microtubules are biopolymer molecules made from tubulin dimer subunits, and in solution, each tubulin monomer is bound by a GTP (guanosine triphosphate) molecule. When these subunits are assembled into the polymer filament, one of these GTP molecules might hydrolyze via a two-stage process that involves GTP cleavage into GDP (guanosine diphosphate) and inorganic phosphate (P_i), which is followed by a slow release of P_i .^{1–3} It has been realized that the hydrolysis is a key process for understanding dynamic processes in microtubules;

however, microscopic details of the process are still controversial.^{13–17} Two main hydrolysis mechanisms for cytoskeleton proteins have been discussed so far. In the random model, the hydrolysis can take place with equal probability at any microtubule subunit.^{18–23} At the same time, in the vectorial model, it is assumed that hydrolysis occurs only at the boundary between GDP-associated subunits (already hydrolyzed) and GTP-associated monomers (not yet hydrolyzed).^{13,16,24,25} In addition, a cooperative hydrolysis mechanism that interpolates between these two limiting pictures has also been proposed and analyzed.^{11,26–28} In this model, the hydrolysis rates are different depending on the local environment of the given subunit. Which mechanism is realized for cytoskeleton proteins is still under discussion;^{17,27,28} however, recent experiments for microtubules⁸ suggest a mechanism more consistent with the random or cooperative hydrolysis models.

One of the main reasons for difficulties in describing cytoskeleton protein dynamics is the fact that most current theoretical views on hydrolysis are thermodynamically inconsistent: existing models are mainly phenomenological, or they neglect free energy change associated with corresponding biochemical processes due to different interactions between

Received: May 15, 2013

Revised: June 28, 2013

Published: July 11, 2013

subunits in these biopolymers. Recent theoretical and experimental studies have found that these interactions are important for understanding growth dynamics of microtubules;^{29,30} however, they are still not taken into account for analyzing hydrolysis processes. In addition, many theoretical models utilize a continuum approach that cannot be used for understanding discrete biochemical and mechanical transitions in microtubules at the level of one or few subunits.¹⁷

In this work, we present a new theoretical approach to understand complex dynamics in microtubules by accounting for most relevant biochemical transitions including tubulin monomer attachments, detachments, and hydrolysis. A new feature in our discrete-state stochastic method is a microscopic physical–chemical description of hydrolysis processes that allows us to consistently determine hydrolysis rates at each subunit depending on the free-energy changes in related chemical transitions. Several dynamic properties of microtubules are calculated using both analytical and computer simulations. The theoretical results are also compared with available experimental observations. In addition, the role of cooperativity in the hydrolysis on microtubule dynamics is discussed.

THEORETICAL METHODS

The microtubule is a hollow cylindrical polymer assembled from GTP–tubulin dimers. It usually contains 13 linear protofilaments arranged in parallel fashion.⁵ In this work, we neglect the protofilament structure, and the microtubule is viewed as a single filament polymer. It has been argued before that despite this simplified view, most dynamic features of microtubules can still be successfully captured.¹⁷ Since the phosphate (P_i) release rate is much slower than the GTP cleavage rate for the GTP hydrolysis process in microtubules, we consider a simplified model where only the second rate-limiting step of hydrolysis is taken into account and tubulin subunits bound to GTP or GDP– P_i are treated to be the same species.¹⁷ Thermodynamic analysis of the system suggests that chemical and mechanical interactions between tubulin subunits in the microtubule might affect hydrolysis processes, leading to different hydrolysis rates depending on configurations of the interface that connects GDP (D) and GTP (T)-subunits, see Figure 1. The fact that the hydrolysis rate depends on the biochemical structure and mechanical properties of the microtubule is a central part of our theoretical method, and it is a new observation that has not been used before in

theoretical modeling of cytoskeleton proteins. To quantify this effect, we need to calculate free energy differences during the individual hydrolysis events. Three different hydrolysis transitions can take place for the single-filament protein as shown in Figure 1. The free-energy difference for the situation described in Figure 1A is given by

$$\Delta G_1 = 2\varepsilon_{TD} - 2\varepsilon_{TT} \quad (1)$$

where we defined ε_{kl} as a free energy of interaction between subunits of type k and l (with k, l being D or T for hydrolyzed and unhydrolyzed subunits, respectively). The coefficient 2 in the free energy expression reflects the fact that during the hydrolysis process for the internal monomer two interfaces are modified. Similarly, the free energy change for the hydrolysis process in Figure 1B is equal to

$$\Delta G_2 = \varepsilon_{DD} - \varepsilon_{TT} \quad (2)$$

Also, for the case presented in Figure 1C, we have

$$\Delta G_3 = 2\varepsilon_{DD} - 2\varepsilon_{TD} \quad (3)$$

From eqs 1–3, it can be shown that the free energy changes can be rewritten in the more convenient way,

$$\Delta G_1 = 2\varepsilon + \Delta G_3, \quad \Delta G_2 = \varepsilon + \Delta G_3 \quad (4)$$

where

$$\varepsilon = 2\varepsilon_{TD} - \varepsilon_{TT} - \varepsilon_{DD} \quad (5)$$

The parameter ε has a physical meaning of relative thermodynamic cost of putting the hydrolyzed subunit in the filament. It can also be seen as a sum of differences in interactions between hydrolyzed and unhydrolyzed subunits, $\varepsilon = (\varepsilon_{TD} - \varepsilon_{DD}) + (\varepsilon_{TD} - \varepsilon_{TT})$. It is known that for any chemical transition, the ratio of forward and backward rates depend on the free energy difference for this transition. Typically, the rate into the state that has a lower free energy is higher. It suggests that the hydrolysis rates for the microtubule can be written as $r_i \approx \exp[-\theta\Delta G_i/(k_B T)]$ with $i = 1, 2$, or 3 and a parameter θ ($0 \leq \theta \leq 1$) specifying a relative distance to a transition state along the reaction coordinate for the hydrolysis process. The parameter θ has also a physical meaning of how the activation barrier for the chemical reaction correlates with the free-energy difference for the transition. Since the thermodynamic energies of states after hydrolysis are different, as shown in Figure 1, the corresponding rates are related via

$$\frac{r_1}{r_3} = \alpha^2, \quad \frac{r_2}{r_3} = \alpha \quad (6)$$

where we define a hydrolysis cooperativity parameter α as

$$\alpha = \exp[-\theta\varepsilon/(k_B T)] \quad (7)$$

Because the hydrolyzed subunits in microtubules dissociate quickly, we expect that $|\varepsilon_{DD}| \approx |\varepsilon_{TD}| \ll |\varepsilon_{TT}|$, that is, two T subunits have the strongest attractive interactions, while two D as well as D and T tubulin monomers interact much more weakly. Then from eq 5, one might conclude that the energy difference $\varepsilon \geq 0$, and the cooperativity parameter α is always between zero and one. It is interesting to consider limiting cases. For $\varepsilon = 0$, that is, $\alpha = 1$, all hydrolysis rates are independent of the local biochemical environment and they become equal, $r_1 = r_2 = r_3 = r$. This is the case known as the random hydrolysis model in the phenomenological theoretical approaches. In another limit, when $\varepsilon \rightarrow \infty$, that is, $\alpha \rightarrow 0$, we have $r_1 \rightarrow 0$ and $r_2 \rightarrow 0$. This suggests that the hydrolysis might

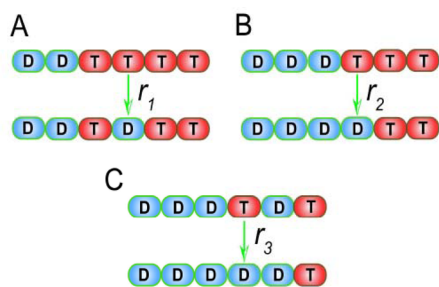


Figure 1. Hydrolysis rates of tubulin–GTP subunits in microtubules: (A) the GTP hydrolysis rate of a tubulin dimer with two neighboring subunits bound to GTP; (B) the GTP hydrolysis rate of a tubulin dimer with one neighboring subunit bound to GTP and the other one bound to GDP; (C) the GTP hydrolysis rate of a tubulin dimer with two neighboring subunits already hydrolyzed.

only happen for subunits surrounded from both sides by already hydrolyzed monomers (see Figure 1C). In this case, any segment of two or more T subunits can never be hydrolyzed. Obviously, for microtubules this is not a realistic situation, and this limit is most probably unphysical. Surprisingly, this limit does not lead to the vectorial hydrolysis model considered in phenomenological approaches as one would expect.

For $0 < \alpha < 1$, the GTP hydrolysis rate for a given subunit is no longer a constant value but it depends on the chemical states of the neighboring monomers because after hydrolysis the corresponding interfaces will be modified. Generally, this situation can be viewed as a cooperative hydrolysis process. The hydrolysis rate r_3 as shown in Figure 1C is probably the largest one, and the cooperativity for the hydrolysis becomes stronger for smaller values of α . The random hydrolysis is observed when there is no cooperativity ($\alpha = 1$). It is important to note that our cooperative hydrolysis mechanism is different from previous theoretical models^{11,27,28} since our microscopic description, in contrast to phenomenological pictures, consistently takes into account all interactions between neighboring subunits. In addition, our method predicts that the hydrolysis rates for terminal subunits differ from the hydrolysis of the internal monomers. It can be shown using free-energy calculations and assuming $|\epsilon_{DD}| \approx |\epsilon_{TD}|$ that the hydrolysis rate for the case when the end subunit is bound to the unhydrolyzed (T) monomer is equal to r_2 , while for the D monomer interacting with the last subunit, it is given by r_3 (see Figure 2).

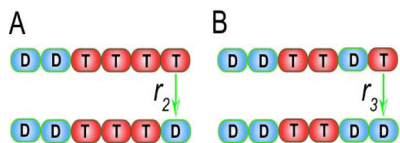


Figure 2. Hydrolysis rates of end subunits: (A) the hydrolysis rate for the end subunit connected to the unhydrolyzed tubulin monomer; (B) the hydrolysis rate of the end subunit connected to the hydrolyzed tubulin monomer.

In addition, we assume that the filament is in the solution that has a constant concentration, C_T , of free tubulin–GTP molecules, and the filament length can increase via the addition of the tubulins with the rate $U = k_{on}C_T$. If the end subunit is in the state T, it can dissociate from the filament with the rate W_T , while the shrinking of the filament when the last subunit is already hydrolyzed is given by the rate W_D . Depending on the position and chemical composition of neighboring monomers, T subunits might hydrolyze with the rates r_1 , r_2 , or r_3 as discussed above (see also Figure 1). Since in microtubules one of the ends (plus end) is much more dynamic than the other one (minus end), for convenience, we analyze filaments with only one active end, although all arguments can be easily extended to microtubules with both active ends. The utilized transition rates are given in Table 1.

Table 1. Parameters for the Chemical Transition Rates for Analyzing Microtubules in Our Model

parameter	rates, s ⁻¹	ref
k_{on} , on-rate of T-tubulin dimer (plus end)	3.2	3
W_T , off-rate of T-tubulin dimer (plus end)	5.5	5
W_D , off-rate of D-tubulin dimer (plus end)	290	3
r , hydrolysis rate [for the case in Figure 1C]	0.2	17

RESULTS AND DISCUSSION

Chemical Composition of Filaments. To understand dynamic processes in microtubules, it is important to determine the chemical states and spatial distributions of all monomers in the protein filament. Our theoretical method allows us to do it quite efficiently. We denote the position of the terminal subunit at the end of filament as $i = 1$, and the subunit i corresponds to the i th monomer in the filament counting from the terminal subunit. Thus our calculations are performed in the reference frame associated with the end monomer. An occupation number, τ_i , is also introduced for each subunit such that $\tau_i = 1$ if the monomer is not hydrolyzed (T state) and $\tau_i = 0$ for the hydrolyzed subunit (D state). Then, the time evolution for the average occupation number, $\langle \tau_i \rangle$, can be estimated from corresponding master equations,

$$\begin{aligned} \frac{d\langle \tau_i \rangle}{dt} = & U\langle \tau_{i-1} - \tau_i \rangle + W_T\langle \tau_i(\tau_{i+1} - \tau_i) \rangle \\ & + W_D\langle (1 - \tau_i)(\tau_{i+1} - \tau_i) \rangle - \alpha^2 r\langle \tau_{i-1}\tau_i\tau_{i+1} \rangle \\ & - \alpha r\langle (1 - \tau_{i-1})\tau_i\tau_{i+1} + \tau_{i-1}\tau_i(1 - \tau_{i+1}) \rangle \\ & - r\langle (1 - \tau_{i-1})\tau_i(1 - \tau_{i+1}) \rangle \end{aligned} \quad (8)$$

where $r_3 = r$ and different hydrolysis processes are taken into account as described in Figure 1. The parameter α here is defined in eq 7 as a measure of cooperativity, and it takes values in the range $0 < \alpha \leq 1$. For the terminal subunit $i = 1$, the average occupation number, $\langle \tau_1 \rangle$ is governed by a different master equation,

$$\begin{aligned} \frac{d\langle \tau_1 \rangle}{dt} = & U\langle 1 - \tau_1 \rangle - W_T\langle \tau_1(1 - \tau_2) \rangle + W_D\langle \tau_2(1 - \tau_1) \rangle \\ & - \alpha r\langle \tau_1\tau_2 \rangle - r\langle \tau_1(1 - \tau_2) \rangle \end{aligned} \quad (9)$$

To solve these equations, we take a mean-field approach and neglect the correlations in occupancies, that is, $\langle \tau_i\tau_j \rangle$ is approximated as $\langle \tau_i \rangle \langle \tau_j \rangle$ for any i and j . For $\alpha = 1$, eqs 8 and 9 are reduced to corresponding master equations in the random hydrolysis model as discussed in detail in ref 17. The recursion relations for $\langle \tau_i \rangle$ under steady state conditions can be obtained by setting the left-hand sides of eqs 8 and 9 equal to zero. For convenience, we define a probability that the terminal subunit is in the T state as $\langle \tau_1 \rangle = q$, and the recursion relations are assumed to have the following solution for $i \geq 1$,

$$\frac{\langle \tau_{i+1} \rangle}{\langle \tau_i \rangle} = b \quad (10)$$

where a constant b can be obtained from solving the algebraic equations after substituting eq 10 into eqs 8 and 9 (see the Supporting Information). For α that is not very small, it can be shown that

$$\begin{aligned} b \approx & \{qr[2q(1 - \alpha) - 1] + [4(U - qW_T)(U - qW_T) \\ & - qr] + q^2r^2[2q(1 - \alpha) - 1]^2\}^{1/2} / [2(U - qW_T)] \end{aligned} \quad (11)$$

For the random hydrolysis mechanism with $\alpha = 1$, eq 11 simplifies into

$$b = \frac{U - q(W_T + r)}{U - qW_T} \quad (12)$$

which is exactly the expression obtained in earlier theoretical studies.¹⁷ The probability, q , can be obtained explicitly as a function of all chemical transition rates from eqs 8–10.^{17,31} The exact expressions for probabilities of different microtubule conformations provides a direct way of estimating all dynamic properties of the system. Specifically, the mean filament growth rate is given by

$$V = [U - W_T q - W_D(1 - q)]d \quad (13)$$

where d is the effective tubulin dimer size, which is equal to $8/13 \approx 0.6$ nm in our model, corresponding to the length of a tubulin dimer divided by the number of protofilaments in the microtubule.

During the assembly process of microtubules, segments of unhydrolyzed T subunits are formed along the filament length, and the last segment with the terminal subunit is called a cap. It is believed that this cap keeps the filament as a stable structure, protecting it from fast depolymerization of hydrolyzed subunits, which is known as a catastrophe event. At large times, the microtubule reaches a stationary state at which the spatial distribution of hydrolyzed and unhydrolyzed subunits can be fully determined. One can define the steady-state probability, P_l , that the cap is composed of exactly l T subunits,¹⁷

$$P_l = \left(\prod_{i=1}^l \langle \tau_i \rangle \right) (1 - \langle \tau_{l+1} \rangle) \quad (14)$$

with $\langle \tau_i \rangle = b^{i-1} q$ from eq 10. Then, the average size, $\langle l \rangle$ of the GTP-cap is given by

$$\langle l \rangle = \sum_{l \geq 1} l P_l = \sum_{l \geq 1} b^{l(l-1)/2} q^l \quad (15)$$

There is a different method of estimating the average size of the GTP-cap under varying conditions. Another mean-field approach for investigating actin filaments dynamics using a phenomenological cooperative hydrolysis mechanism has been developed recently.³² This is a continuum method, and it only works for fast growth rates. Adopting it for our model of microtubule dynamics with more microscopic description of hydrolysis leads to the following expression under high tubulin concentration, C_T , in the solution,

$$\langle l \rangle \approx \sqrt{\frac{\pi}{2}} \sqrt{J_T/r} \frac{1}{\alpha} \quad (16)$$

where the function J_T is the assembly rate of the filament (See the Supporting Information for more details). The expression for J_T is simply given by $J_T = U_T - W_T$ for large C_T . Equation 16 shows that the average size of the GTP-cap increases as the square root of the growth rate, but it is inversely proportional to the square root of the hydrolysis rate r , which are the same as the conclusions obtained for the more phenomenological cooperative hydrolysis model that considered only one neighboring subunit effect.³² However, the dependence of the average size of the GTP-cap on the cooperativity parameter α is different in each methods.

The average size of the GTP-cap as a function of tubulin dimer concentration C_T is shown in Figure 3 for different values of the cooperative parameter α and for the experimentally measured chemical transition rates summarized in Table 1. The figure shows that increasing the cooperativity (lowering α) makes the length of the GTP-cap significantly larger for the tubulin concentrations above the critical, while below the critical concentration, the cooperative effect does not influence

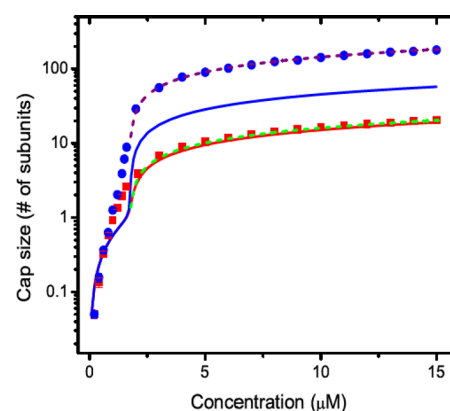


Figure 3. Average size of the GTP-cap as a function of the free tubulin concentration, C_T , in μM . The red ($\alpha = 0.9$) and blue ($\alpha = 0.1$) solid lines are the mean-field analytical solutions given by eq 15, and the green ($\alpha = 0.9$) and violet ($\alpha = 0.1$) dashed lines are given by eq 16 from another mean-field analytical method. The red squares ($\alpha = 0.9$) and blue circles ($\alpha = 0.1$) are simulation results.

the cap length. These observations could be easily explained by analyzing master eqs 8 and 9. For smaller α , the probability to hydrolyze subunits in the microtubule filaments effectively decreases, and it is important for tubulin concentrations above the critical concentration when the relatively large stable cap exists. For concentrations below the critical concentration, the cap is unstable and very small, and this effect is weaker. Similar effects are found for other dynamic properties of microtubules. This is an important observation because it suggests a possible experimental way of measuring the cooperativity parameter α that might help in uncovering microscopic details of the hydrolysis mechanism in microtubules. Our suggestion is the following: at low tubulin concentrations, our theory predicts that the cooperativity does not play a role, so at these conditions, one might extract the hydrolysis rate r from experimental data. At the same time, for large tubulin concentrations, the cooperativity effect should play a role, and it can be obtained directly by utilizing eq 15 or eq 16 from measurements of the cap length or from other measured properties of microtubules.

In Figure 3, we also compare the predictions from two different mean-field approximations with numerically exact calculations obtained via computer Monte Carlo simulations. When the cooperativity during the hydrolysis processes is not large ($\alpha = 0.9$), both mean-field theories show an excellent agreement with exact calculations. The situation is different for strong cooperativity conditions when α is small. Here the continuum mean-field approach [eq 16] also agrees well with the simulations, while the predictions of the discrete mean-field theory [eq 15] are only qualitatively correct. However, the continuum mean-field method can only be utilized above the critical concentration, while the discrete theory works for all tubulin concentrations. The deviations between mean-field approximations and exact solutions are obviously because correlations in the chemical composition of microtubule subunits are neglected in the mean-field pictures. Increasing the cooperativity in the hydrolysis processes apparently leads to stronger correlations in nucleotide composition of microtubule filaments.

Frequency of Catastrophes. Dynamic instability in microtubules is one of the most fundamental processes that controls and regulates many cellular activities.^{1–3,33} Despite

multiple years of experimental and theoretical studies, the fundamental mechanisms of this phenomenon remain unclear. It is important to go beyond the simplest phenomenological description to understand the underlying microscopic nature of dynamic instability. Our thermodynamically consistent theoretical approach that takes into account most important biochemical and mechanical processes is well suited for analyzing microscopic events during dynamic instability. It is known that microtubules can be found in one of two dynamic phases: in growing phase, the filament length increases, while in the shrinking phase, it decreases. The transitions between these two dynamic phases are called catastrophes and rescues, respectively. Since in our approach all chemical states of microtubule subunits can be explicitly described, it is a convenient way of analyzing the dynamic instability. Following earlier theoretical suggestions,^{12,17} a shrinking dynamic phase is defined as a set of configurations with the last N subunits of the microtubule being in the hydrolyzed state independently of the chemical states of other subunits in the filament. This reflects the fact that hydrolyzed monomers dissociate fast from the filament. The rest of microtubule configurations belong to the growing dynamic phase since they typically have a protective cap of T subunits that depolymerize quite slowly and the biopolymer mostly grows via addition of tubulin–GTP molecules from the solution. It is important to note that in contrast to some phenomenological models, our approach can be applied for all tubulin concentrations and it naturally accounts for both catastrophes and rescues.¹⁷

We define a catastrophe frequency, $f_c(N)$, as the inverse of the mean time that the system stays in the growing phase. It can be calculated as a total flux out of the growing phase into the shrinking phase configurations.¹⁷ For $N = 1$, which means that in the shrinking phase there is at least one terminal D subunit, the flux arguments produce the following result for the frequency of catastrophes (see the Supporting Information):

$$f_c(1) = W_T(1 - bq) + r - (1 - \alpha)brq \quad (17)$$

The corresponding expressions for other values of $N > 1$ can also be obtained analytically as shown in the Supporting Information. The first two terms on the right side of eq 17 are the same as for the random hydrolysis model,¹⁷ while the third term is a result of cooperativity in the hydrolysis processes. The important result here is that the cooperativity in the hydrolysis reduces the frequency of catastrophes. The microtubule configurations in the shrinking phase have hydrolyzed subunits at the end of the filament, but the cooperativity lowers the probability of hydrolysis of T subunits at the end [see Figure 2 and eq 6], leading to reduced catastrophe rates.

In Figure 4, the predicted values of the catastrophe frequency as a function of the growth velocity of filaments is compared with experimental results. The solid line is obtained from our theoretical model with the parameter values listed in Table 1 and for $N = 2$. The symbols correspond to experimental data.³⁴ The analysis of the Figure 4 suggests that experimental observations of catastrophes in microtubules can be well explained by the model with a weak cooperativity in GTP hydrolysis ($\alpha = 0.9$). It is intriguing to note that recent theoretical and computational studies of actin filaments suggest a strongly cooperative hydrolysis.³⁵ These observations agree with known experimental results, and they can also be well explained from our theoretical views [see eq 17]. For microtubules, the cooperativity is weak, and catastrophes are frequently observed leading to dynamic instability. In actin

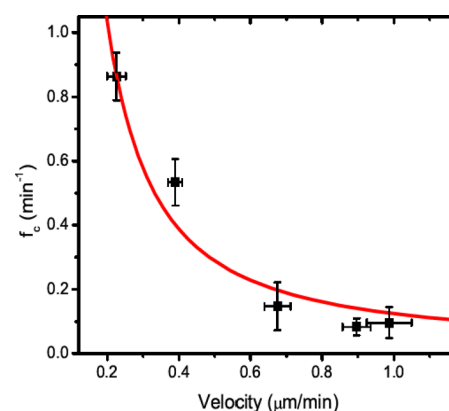


Figure 4. Catastrophe frequency, f_c , versus growth velocity of microtubules. Experimental data from ref 34 (squares with error bars) is compared with our mean-field theoretical calculations (solid line). The values of model parameters are shown in Table 1 with the cooperativity factor $\alpha = 0.9$ and $N = 2$.

filaments, the strong cooperativity effectively blocks the catastrophes, and dynamic instability is not observed.

The role of the cooperativity in the hydrolysis is also analyzed in Figure 5A where the catastrophe frequencies as a

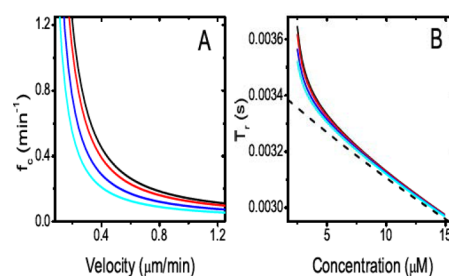


Figure 5. (A) Catastrophe frequency versus growth velocity of microtubules for varied values of α and $N = 2$. (B) Rescue time versus free tubulin concentration, C_T , for varied values of α and $N = 2$. The black, red, blue, and cyan lines correspond to $\alpha = 1.0, 0.9, 0.7,$ and 0.5 , respectively. The dashed line in panel B is given by eq 19.

function of growth velocity of the microtubule are presented for different cooperativity parameters α . One can clearly see that increasing the cooperativity in hydrolysis lowers the rate of transition into the shrinking dynamic phase, and for faster growing microtubules, the catastrophe frequency decreases. It can be explained by the fact that for large velocities the cap of unhydrolyzed subunits is large and to transition into the shrinking phase N terminal T subunits must be hydrolyzed, which is difficult since new T monomers are constantly added at a high rate. For slow growing microtubules, the cap is typically small, and the catastrophe might start not only from the hydrolysis but also from the dissociation of the end T subunits, while the addition of new tubulin monomers is slow.

Rescue Times. An important aspect of dynamic instability phenomena is its reversibility: shrinking microtubules might stochastically reverse back into the growing phase in the process known as a rescue. One of the advantages of our theoretical approach is that the statistics of rescues can be explicitly evaluated. Using flux arguments similar to those used in the analysis of catastrophes, one can show that the frequency of rescues is given by

$$f_r(N) = U + W_D b^N q \quad (18)$$

which is formally the same as the expression obtained for the random hydrolysis model¹⁷ (see the Supporting Information for details). But note that the cooperativity in hydrolysis influences the rescues because the parameter q , which is the probability that the end subunit is unhydrolyzed, depends on the cooperativity parameter α [see eq 11].

The first term at the right-hand side of eq 18 is from adding one GTP–tubulin dimer to the filament from the solution, and the second term reflects the detachment of N hydrolyzed subunits until the appearance of the T subunit at the terminal position, which transfers the filament into the growing phase. The time that a microtubule spends in the shrinking phase, $T_r(N) = 1/f_r(N)$, is known as a rescue time, and it is plotted in Figure 5B as a function of the tubulin concentration for different values of the cooperativity parameter α . The rescue time decreases as the tubulin concentration increases, which is caused by the larger assembly rate of GTP–tubulin dimers at higher concentrations as well as by the increase in the parameter q . Comparing rescue times for different values of α indicates that the cooperativity lowers the rescue times, and the effect is essentially negligible for larger tubulin concentrations. One could argue that this happens because the cooperativity in hydrolysis decreases the possibility of hydrolyzing internal subunits in the microtubule. This, in turn, leads to larger probability to be rescued by incoming GTP–tubulin subunits from the solution. More specifically, it has been shown before that larger sizes of the cap can be obtained for stronger cooperativity (see Figure 3). Therefore, the probability q for the terminal subunit to be unhydrolyzed will also increase as α becomes smaller. Equation 18 indicates that the rescue time will decrease as the value of q increases. For large tubulin concentrations, we always have $q \approx 1$, and no dependence on the cooperativity is observed. It can be shown that in this limit the rescue times can be written as

$$T_r(N) = \frac{1}{U + W_D} \quad (19)$$

as presented by the dashed line in Figure 5B. It is interesting to note also that the relative effect of the cooperativity in hydrolysis on rescues is smaller than the effect on the catastrophes. This is a result of large contributions of GTP–tubulin associations to the rescue processes, in contrast to the catastrophes, which are controlled by hydrolysis and dissociations.

SUMMARY AND CONCLUSIONS

In this work, we developed a new theoretical method of analyzing dynamic processes in microtubules. Our discrete-state stochastic models take into account the most important biochemical transitions such as associations and dissociations of tubulin subunits, as well as hydrolysis processes inside of the biopolymer molecule. Since the hydrolysis plays a critical role in microtubule dynamics, in our theory we adopted a more microscopic physical–chemical treatment of the hydrolysis processes. It is argued that rates of hydrolysis processes depend on the chemical composition of monomers and they are estimated via free-energy differences for involved transitions. This approach allows us to fully quantify the effect of cooperativity in hydrolysis.

First, our theoretical method with more thermodynamically consistent evaluation of hydrolysis processes is compared with

available phenomenological models of hydrolysis. It is shown that when there is no cooperativity the phenomenological random model of the hydrolysis, in which all hydrolysis rates are the same, is recovered. However, another widely utilized vectorial model, when the hydrolysis can only take place at the interface between T and D subunits, cannot be obtained in our approach. This leads to an important conclusion that the vectorial model is probably *unrealistic* to use for analysis of cytoskeleton protein dynamics since it does not have strong physical–chemical foundations. This might also be related to the existing controversy on what hydrolysis mechanisms describe better experimental measurements on actin filaments and microtubules.

Theoretical calculations in our model are utilized to analyze dynamic properties of microtubules. It is shown that above the critical concentration the length of the GTP-cap increases for stronger cooperativity in hydrolysis processes because of the lower probability of hydrolyzing T subunits. However, for conditions below the critical concentration, the cooperativity does not affect the cap length since the cap is smaller and less stable and its length is mostly controlled via subunit dissociations. Similar trends are observed for other dynamic properties of microtubules. It allows us to propose a possible experimental way of estimating hydrolysis rates and the degree of cooperativity by analyzing separately dynamics above and below the critical concentration.

Finally, the developed theoretical approach is applied for analyzing dynamic instability phenomena in microtubules. The advantage of our theory is the fact that it can simultaneously describe both catastrophes and rescues. It is found that increasing the cooperativity in hydrolysis lowers the frequency of catastrophes since the effective hydrolysis rate for terminal subunits is lower. We also present theoretical calculations and computer simulations to argue that the frequency of rescue events is larger for stronger cooperativity in hydrolysis. Comparing theoretical predictions with available experimental data, the degree of cooperativity for microtubules is estimated to be very low, while the cooperativity of hydrolysis in actin filaments is indicated to be quite strong. This leads us to a suggestion that the degree of cooperativity strongly correlates with the existence of dynamic instability in cytoskeleton filaments: for weak cooperativity, dynamic instability is observed, and this is the case for microtubules; for strong cooperativity in hydrolysis, catastrophes are suppressed and dynamic instability is not observed as found for actin filaments.

Although the presented theoretical model captures most properties of complex dynamics of microtubules, as shown by analytical calculations, computer simulations, and comparison with experimental data, the approach is rather oversimplified. One of the weakest points of our method is neglecting the multifilament structure of microtubules, since it will also introduce lateral interactions that are important.^{29,30,36} In addition, the microscopic physical–chemical calculations have been applied only for hydrolysis, while similar arguments should be also relevant for other chemical transitions such as associations and dissociations. Furthermore, our mean-field calculations ignore correlations in chemical compositions of microtubule subunits, which might affect dynamic properties of filaments. It will be important to develop more realistic theoretical models of cytoskeleton proteins in order to better understand the foundations of their complex dynamic behavior.

■ ASSOCIATED CONTENT

● Supporting Information

Detailed calculations and derivations for some quantities. This material is available free of charge via the Internet at <http://pubs.acs.org>.

■ AUTHOR INFORMATION

Corresponding Author

*E-mail: tolya@rice.edu. Phone: +1 713 3485672. Fax: +1 713 3485155.

Notes

The authors declare no competing financial interest.

■ ACKNOWLEDGMENTS

The work was supported by a grant from the Welch Foundation (Grant C-1559).

■ REFERENCES

- (1) Alberts, B.; Johnson, A.; Lewis, J.; Raff, M.; Roberts, K.; Walter, P. *Molecular Biology of the Cell*, 4th ed.; Garland Science: New York, 2002.
- (2) Lodish, H.; Berk, A.; Zipursky, S. L.; Matsudaira, P.; Baltimore, D.; Darnell, J. *Molecular Cell Biology*, 4th ed.; W.H. Freeman and Company: New York, 2000.
- (3) Howard, J. *Mechanics of Motor Proteins and the Cytoskeleton*; Sinauer Associates: Sunderland, MA, 2001.
- (4) Howard, J.; Hyman, A. A. *Nature* **2003**, *422*, 753–758.
- (5) Desai, A.; Mitchison, T. J. *Annu. Rev. Cell Dev. Biol.* **1997**, *13*, 87–117.
- (6) Kerssemakers, J. W. J.; Munteanu, L.; Laan, L.; Noetzel, T. L.; Janson, M. E.; Dogterom, M. *Nature* **2006**, *442*, 709–712.
- (7) Schek, H. T.; Hunt, A. *Curr. Biol.* **2007**, *17*, 1445–1455.
- (8) Dimitrov, A.; Quesnoit, M.; Moutel, S.; Cantaloube, I.; Pous, C.; Perez, F. *Science* **2008**, *322*, 1353–1356.
- (9) Hill, T. L. *Proc. Natl. Acad. Sci. U. S. A.* **1984**, *81*, 6728–6732.
- (10) Bayley, P. M.; Schilstra, M. J.; Martin, S. R. *FEBS Lett.* **1989**, *259*, 181–184.
- (11) Flyvbjerg, H.; Holy, T. E.; Leibler, S. *Phys. Rev. Lett.* **1994**, *73*, 2372–2375.
- (12) Brum, L.; Rupp, B.; Ward, J. J.; Nedelec, F. J. *Proc. Natl. Acad. Sci. U. S. A.* **2009**, *106*, 21173–21178.
- (13) Stukalin, E. B.; Kolomeisky, A. B. *Biophys. J.* **2006**, *90*, 2673–2685.
- (14) Zong, C.; Lu, T.; Shen, T.; Wolynes, P. G. *Phys. Biol.* **2006**, *3*, 83–92.
- (15) Antal, T.; Krapivsky, P. L.; Redner, S.; Mailman, M.; Chakraborty, B. *Phys. Rev. E.* **2007**, *76*, No. 041907.
- (16) Ranjith, P.; Lacoste, D.; Mallick, K.; Joanny, J. F. *Biophys. J.* **2009**, *96*, 2146–2159.
- (17) Padinhateeri, R.; Kolomeisky, A. B.; Lacoste, D. *Biophys. J.* **2012**, *102*, 1274–1283.
- (18) Ohm, T.; Wegner, A. *Biochim. Biophys. Acta* **1994**, *1208*, 8–14.
- (19) Blanchoin, L.; Pollard, T. D. *Biochemistry* **2002**, *41*, 597–602.
- (20) Bindschadler, M.; Osborn, E. A.; Dewey, C. F.; McGrath, J. L. *Biophys. J.* **2004**, *86*, 2720–2739.
- (21) Vavylonis, D.; Yang, Q.; O’Shaughnessy, B. *Proc. Natl. Acad. Sci. U. S. A.* **2005**, *102*, 8543–8548.
- (22) VanBuren, V.; Odde, D. J.; Cassimeris, L. *Proc. Natl. Acad. Sci. U. S. A.* **2002**, *99*, 6035–6040.
- (23) Erenkamper, C.; Kruse, K. *Phys. Biol.* **2009**, *6*, No. 046016.
- (24) Pantaloni, D.; Hill, T. L.; Carlier, M. F.; Korn, E. D. *Proc. Natl. Acad. Sci. U. S. A.* **1985**, *82*, 7207–7211.
- (25) Korn, E. D.; Carlier, M. F.; Pantaloni, D. *Science* **1987**, *238*, 638–644.
- (26) Pieper, U.; Wegner, A. *Biochemistry* **1996**, *35*, 4396–4402.
- (27) Li, X.; Kierfeld, J.; Lipowsky, R. *Phys. Rev. Lett.* **2009**, *103*, No. 048102.
- (28) Burnett, M. M.; Carlsson, A. E. *Biophys. J.* **2012**, *103*, 2369–2378.
- (29) Stukalin, E. B.; Kolomeisky, A. B. *J. Chem. Phys.* **2004**, *121*, 1097–1104.
- (30) Gardner, M. K.; Charlebois, B. D.; Janosi, I. M.; Howard, J.; Hunt, A. J.; Odde, D. J. *Cell* **2011**, *146*, 582–592.
- (31) Padinhateeri, R.; Mallick, K.; Joanny, J. F.; Lacoste, D. *Biophys. J.* **2010**, *98*, 1418–1427.
- (32) Li, X.; Lipowsky, R.; Kierfeld, J. *Europhys. Lett.* **2010**, *89*, 38010.
- (33) Mitchison, T.; Kirschner, M. *Nature* **1984**, *312*, 237–242.
- (34) Drechsel, D. N.; Hyman, A. A.; Cobb, M. H.; Kirschner, M. W. *Mol. Biol. Cell* **1992**, *3*, 1141–1154.
- (35) Janson, M. E.; de Dood, M. E.; Dogterom, M. *J. Cell Biol.* **2003**, *161*, 1029–1034.
- (36) Son, J.; Orkoulas, G.; Kolomeisky, A. B. *J. Chem. Phys.* **2005**, *123*, No. 124902.